

ACCEPTED MANUSCRIPT • OPEN ACCESS

Minimalist analogue robot discovers animal-like walking gaits.

To cite this article before publication: Benjamin John Henry Smith *et al* 2019 *Bioinspir. Biomim.* in press <https://doi.org/10.1088/1748-3190/ab654e>

Manuscript version: Accepted Manuscript

Accepted Manuscript is “the version of the article accepted for publication including all changes made as a result of the peer review process, and which may also include the addition to the article by IOP Publishing of a header, an article ID, a cover sheet and/or an ‘Accepted Manuscript’ watermark, but excluding any other editing, typesetting or other changes made by IOP Publishing and/or its licensors”

This Accepted Manuscript is © 2019 IOP Publishing Ltd.

As the Version of Record of this article is going to be / has been published on a gold open access basis under a CC BY 3.0 licence, this Accepted Manuscript is available for reuse under a CC BY 3.0 licence immediately.

Everyone is permitted to use all or part of the original content in this article, provided that they adhere to all the terms of the licence <https://creativecommons.org/licenses/by/3.0>

Although reasonable endeavours have been taken to obtain all necessary permissions from third parties to include their copyrighted content within this article, their full citation and copyright line may not be present in this Accepted Manuscript version. Before using any content from this article, please refer to the Version of Record on IOPscience once published for full citation and copyright details, as permissions may be required. All third party content is fully copyright protected and is not published on a gold open access basis under a CC BY licence, unless that is specifically stated in the figure caption in the Version of Record.

View the [article online](#) for updates and enhancements.

Minimalist analogue robot discovers animal-like walking gaits

Benjamin J. H. Smith and James R. Usherwood

Royal Veterinary College, London, UK

Abstract:

Robots based on simplified or abstracted biomechanical concepts can be a useful tool for investigating how and why animals move the way they do. In this paper we present an extremely simple quadruped robot, which is able to walk with no form of software or controller. Instead, individual leg movements are triggered directly by switches on each leg which detect leg loading and unloading. As the robot progresses, pitching and rolling movements of its body result in a gait emerging with a consistent leg movement order, despite variations in stride and stance time. This gait has similarities to the gaits used by walking primates and grazing livestock, and is close to the gait which was recently theorised to derive from animal body geometry. As well as presenting the design and construction of the robot, we present experimental measurements of the robot's gait kinematics and ground reaction forces determined using high speed video and a pressure mat, and compare these to gait parameters of animals taken from literature. Our results support the theory that body geometry is a key determinant of animal gait at low speeds, and also demonstrate that steady state locomotion can be achieved with little to no active control.

1. Introduction:

The gaits that quadrupedal animals use have been a source of fascination for researchers for centuries, both from the perspective of biology and legged robotics. Understanding why animals use the gaits they do can reveal what parameters are selected for in legged locomotion, and may therefore lead to better

1
2
3 24 treatments for gait disorders due to age or pathologies, and enable more robust and efficient walking
4
5 25 and running robots.
6
7

8 26 A gait cycle is divided into the stance phase, where a foot is in contact with the ground, and the swing
9
10 27 phase, where the foot is lifted and moved to the next position. Following Hildebrand [1], gaits can be
11
12 28 categorised into symmetric, where the left and right feet of a pair move alternately (e.g. walking or
13
14 29 trotting), and asymmetric, where the left and right feet move at approximately the same time (e.g.
15
16 30 galloping or bounding). Symmetric gaits can be described using two quantities: duty factor; the
17
18 31 proportion of the stride for which each foot is on the ground, and phase; the timing of the beginning of
19
20 32 stance of a forefoot relative to the beginning of stance of the hind foot on the same side. For example,
21
22 33 in a running trot the duty factor is < 0.5 (since the animal is completely off the ground for a proportion
23
24 34 of the stride), and the stance and swing phases of diagonal pairs of legs are synchronised so the phase is
25
26 35 50%. . It is generally agreed that gaits are linked to speed; typically, quadrupeds walk at low speeds, and
27
28 36 transition to a trot and finally a gallop as their speed increases [2]. However, the mechanisms which
29
30 37 determine which gaits are used in a particular situation, and how and why animals transition between
31
32 38 gaits, are still poorly understood. Some animals, such as small rodents which use a running walk
33
34 39 throughout most of their speed range [3], do not appear to have a strong relationship between their
35
36 40 speed and their gait. Some species use rare or alternative gaits, such as camelids which pace at speeds
37
38 41 where most animals might trot [4], or primates which use diagonal sequence walks where most animals
39
40 42 would use a lateral sequence walk [5]. Conversely, some animals appear to avoid particular types of
41
42 43 gait, such as gnu which transition directly from walking to cantering [6]. Some animals even use
43
44 44 different gaits at different points in their lives, such as macaques, which have been observed to use
45
46 45 lateral sequence walks when young, and shift to diagonal sequence as they age [7].
47
48
49
50
51
52
53
54
55
56
57
58
59
60

1
2
3 46 Both physical and neurological mechanisms have been proposed for why gaits are selected and how
4
5 47 animals transition between gaits [8][9]. One of the most popular theories is that quadrupedal animals
6
7 48 select the gait which is energetically optimal at a given speed [10]; energy cost for a gait changes in a
8
9 49 curvilinear way with speed, thus animals will switch gaits at the speeds where the energy curves for
10
11 50 different gaits intersect, moving to whichever gait will minimise energetic cost. Recently, an energetic
12
13 51 explanation has also been proposed for the phases used by walking quadrupeds[11]; the duty factor
14
15 52 used by the animal determines the relative directions of the centre of mass velocity and the limb forces,
16
17 53 and hence whether it is more economical to reduce vertical centre of mass velocity by distributing
18
19 54 footfalls evenly through time (i.e. a phase of 25% or 75%) or to increase vertical centre of mass velocity
20
21 55 with footfalls that occur close together (i.e. a phase closer to 50%). This is in contrast to previous
22
23 56 stability based explanations for leg phasing during walking, which suggested that quadrupeds attempt to
24
25 57 optimise their support polygon by avoiding situations where they would only be supported by two limbs
26
27 58 [12]. As with bipeds, inverted pendulum dynamics impose an upper limit on the speed quadrupeds can
28
29 59 walk before switching to a running gait [13]. Unlike bipeds, however, many quadrupeds exhibit a second
30
31 60 gait transition from trotting to cantering or galloping; it has been suggested that this is because animals
32
33 61 select the gait which minimises peak forces on the musculoskeletal system, and thus reduce the chance
34
35 62 of injury [14]; peak forces tend to increase with speed in running, however there is a discontinuous drop
36
37 63 in peak force when a quadruped switches from a trot to a gallop[15]. Recently, an alternative theory has
38
39 64 been proposed for the trot-canter transition [16]; animals select gaits to avoid energetically
40
41 65 disadvantageous pitching motions about their centre of mass.
42
43
44
45
46
47
48

49 66 As well as these mechanical explanations, a number of researchers[17][18][19] have also proposed that
50
51 67 gaits can be modelled in terms of oscillator dynamics, with limb phasing and transitions between gaits
52
53 68 emerging from the neural or software interactions of the oscillators. The biological basis for this model
54
55 69 comes from work by Brown [20], who found that hindlimb rhythmic motor activity does not require
56
57
58
59
60

1
2
3 70 sensory input. Later work by Grillner [21] found that sensory input can tune Central Pattern Generators
4
5 71 (CPGs), but does not necessarily drive them, while Duysens and Pearson [22] found that applying a load
6
7 72 to a leg can prolong the stance phase for an indeterminate length of time. One example of how this
8
9 73 model can be implemented is given by Fukuoka, Habu and Fukui [23], using a computer model of a
10
11 74 quadruped robot with a CPG controlling each leg. These CPGs were connected by fixed couplings which
12
13 75 had been tuned to achieve a steady trot; however, the CPGs could be adapted with feedback from force
14
15 76 sensors on the model's feet, which inhibited the leg from transitioning from stance to swing phase while
16
17 77 the leg was loaded. This model was able to exhibit a range of gaits at different speeds, including walking,
18
19 78 trotting and galloping, and transitions between the gaits. The researchers concluded that the pitch and
20
21 79 roll of the body caused a difference in load between the legs of a diagonal pair; specific gaits are caused
22
23 80 by a particular combination of body posture and speed. A similar principle was used by Maufroy,
24
25 81 Nishikawa and Kimura [24] to control both locomotion and posture in both a modelled and real
26
27 82 quadruped robot; each leg had its own independent CPG based controller, which set the leg into the
28
29 83 stance phase when it was loaded, and into the swing phase when it was unloaded. Using identical
30
31 84 parameters for all the legs resulted in a pace gait, where ipsilateral front and rear legs moved at the
32
33 85 same time; incorporating a delay into the fore leg controllers resulted in a diagonal sequence walk,
34
35 86 where a contralateral forefoot moved after a hind foot. Although the robot was originally designed with
36
37 87 no interleg co-ordination, it was found to be sensitive to lateral perturbations, so an ascending co-
38
39 88 ordination mechanism was implemented. The combination of CPGs and sensor inputs has also been
40
41 89 used to improve robustness, with sensor inputs acting as reflexes which tuned the CPG to adapt to
42
43 90 different situations; such as [25], where reflexes were used to tune a CPG to prevent stumbling over
44
45 91 obstacles, and rolling on slopes.

52
53 92 Owaki et al. [26] showed that the couplings between oscillators do not have to be encoded in the
54
55 93 controller, and can instead be physical connections due to the body of an animal or robot, which they

1
2
3 94 described as ‘physical communication’. They constructed a quadruped robot controlled using a central
4
5 95 pattern generator (CPG) formed by four decoupled oscillators, one on each leg. A force sensor on each
6
7 96 leg provided feedback to the oscillator, which was used to determine its phase. This robot, and its
8
9
10 97 subsequent developments, was able to move with animal-like gaits, and carry out speed dependent gait
11
12 98 transitions, despite the lack of centralised control [27]. As well as demonstrating that physical
13
14 99 communication could be used to produce a quadruped gait in the absence of neurological coupling,
15
16 100 these robots were also able to adapt to different loading configurations which changed the position of
17
18 101 the centre of mass, by using different gaits, such as switching from lateral sequence to diagonal
19
20 102 sequence walking. This suggests that body geometry plays a role in which gait is used. More recent
21
22 103 research has found that the interdependence of body geometry and gait also extends to body bending;
23
24 104 optimal gaits were discovered in a salamander-like robot when body flexion and leg occur in
25
26 105 synchronisation[28]. The roles of other physical properties of a robot’s structure in determining gait
27
28 106 have also been investigated, in particular compliance. The goal in [29] was to achieve fast stable
29
30 107 locomotion via open loop compliant stabilization; this was achieved by adapting limb stiffness to speed
31
32 108 in real time to follow the Spring Loaded Inverted Pendulum (SLIP) model, where minimum leg length
33
34 109 was at midstance. This allowed the robot ‘Cheetah-cub’ to run stably at 6.9 body lengths per seconds,
35
36 110 and traverse discontinuous terrain without needing any direct adaptation of its CPG controller. A similar
37
38 111 concept known as ‘embodied computing’ was used in[30] to simplify the control of a quadruped robot;
39
40 112 control signals were directly related to sensor inputs, via non-linear transforms which the robot learned
41
42 113 in real time, and control was outsourced to compliant structural elements rather than a processor. This
43
44 114 enabled the robot to discover stable trotting and walking gaits within a few strides.
45
46
47
48
49
50

51 115 The system presented here takes the principle of body structure affecting gait and extends it to a system
52
53 116 in which gait is determined purely by body geometry, with no controlling oscillators or CPG. This is based
54
55 117 on a recent paper which proposed that animals such as horses and sheep use a specific ‘grazing gait’
56
57
58
59
60

1
2
3 118 while foraging, with a footfall timing which emerges naturally from their body geometry [31]. The
4
5 119 locomotion used during grazing differs from normal walking in that it has a duty factor approaching 1,
6
7 120 rather than around 0.65, and a phase close to (but not exactly) 50%, rather than 25%. The intermittent
8
9 121 nature of grazing requires the animal to move between postures that are statically stable (i.e. with at
10
11 122 least three feet on the ground so that the centre of mass falls within the polygon of support), whereas
12
13 123 the more dynamic nature of continuous gaits allows the animal to support itself on only two or one legs.
14
15 124 Very slow walking, with a duty factor > 0.75 , can achieve this stability requirement by moving a forefoot
16
17 125 immediately after the ipsilateral hindfoot; however, this results in discontinuities in weight support,
18
19 126 which may require corrections which are disadvantageous in terms of energy or stability. Instead,
20
21 127 grazing animals move a foot when it is maximally unloaded; a gait which represents a local, rather than
22
23 128 global minimum in terms of work, but which also minimises any disruption in weight support.

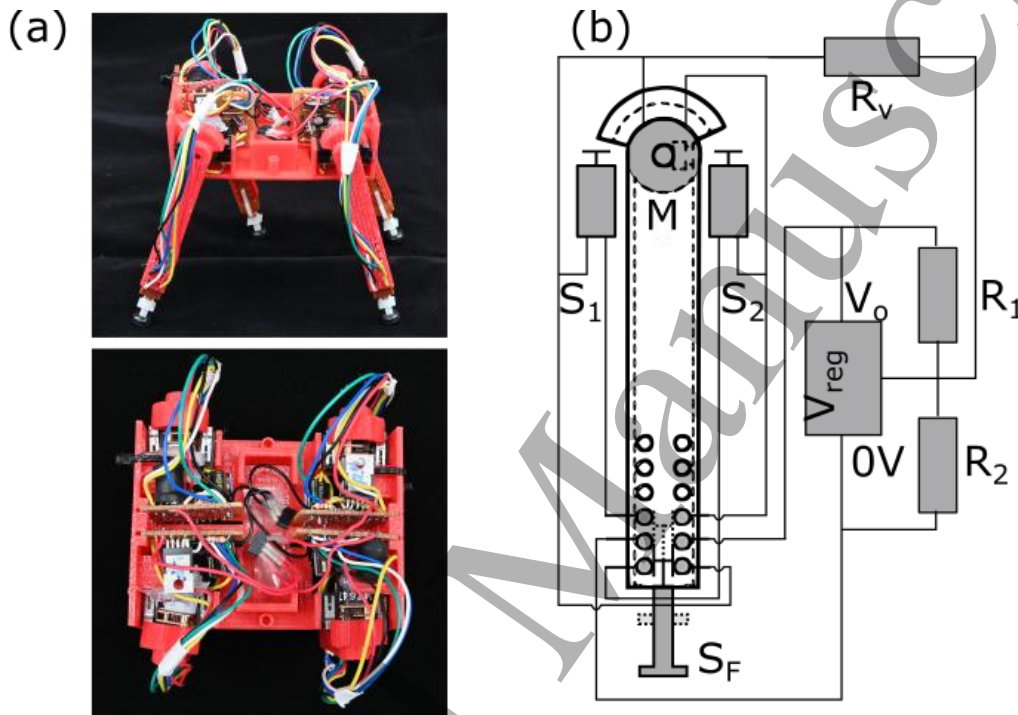
24
25
26
27
28 129 The grazing gait may be of interest to engineers interested in designing robots for moving intermittently
29
30 130 over large areas, for example when surveying for minerals, or minesweeping; if low level locomotion
31
32 131 control can be achieved with little to no computational effort then more processing power will be
33
34 132 available for sensing and path planning. In a more general sense it adds further information to the
35
36 133 discussion about the extents to which animal gaits are determined by neurological or mechanical
37
38 134 structures.

135 **2. Methods:**

136 *2.1 Robot design:*

137 In order to replicate the model in [31] as closely as possible, the robot structure should meet the
138 following assumptions: firstly, the hip and shoulder should vault from low to high then back to low again
139 over the course of a stance; this requires constant leg length during the stance phase (i.e. no knee or
140 ankle joints). Secondly, the shoulders and hips should be connected with a rigid, table top like linkage,

1
2
3 141 which resists bending and twisting. The robot therefore consists of a rectangular body and four legs,
4
5 142 each with one degree of freedom. Figure 1(a) shows a photo of the robot; it is 93mm long, 92mm wide
6
7 143 (including the legs), stands 102mm tall and weighs 220.1g. More detailed mechanical and electronic
8
9 144 plans can be found in the supplementary information S1.1 and S1.2.



35 145
36
37
38 146 *Figure 1: Robot design. (a): A photograph of the completed robot. Each of the legs is fitted with a hard*
39
40 147 *rubber foot to aid traction. (b): Simplified leg circuit. The switch S_F determines the direction the motor M*
41
42 148 *rotates, the switches S_1 and S_2 are limit switches, and the speed of rotation is determined by the output*
43
44 149 *of the voltage regulator V_{reg} , which is a function of the values of R , R_1 and R_2 .*

45
46
47
48 150 In order to demonstrate that biologically plausible locomotion can emerge primarily from the
49
50 151 mechanical configuration of an animal with little to no neurological input, it was decided to build an
51
52 152 analogue robot, controlled using analogue electronics rather than a digital microprocessor. Analogue
53
54 153 robots include BEAM (Biology, Electronics, Aesthetics and Mechanics), or Biomorphic robots [32], which

1
2
3 154 attempt to achieve biological- like reactions to stimuli using simple analogue circuits, and Braitenberg
4
5 155 vehicles [33] which produce apparently complex behaviours such as exploring based purely on sensor
6
7 156 inputs. These types of systems were particularly popular in the early days of robotics, when the size of
8
9 157 computers made more complex on board controllers unfeasible; however, the close links between
10
11 158 sensors and actuators with minimal interposition of software also makes them an interesting model of
12
13 159 low level biological control. Still and Tilden demonstrated an analogue quadruped robot which was able
14
15 160 to walk with no software [34]. Instead, control was provided using a ring of four coupled oscillators,
16
17 161 each implemented using an inverter and a resistor-capacitor (RC) high pass filter. This network produced
18
19 162 two different modes of oscillation, which translated to two different gaits: a walk like gait and a trot like
20
21 163 gait; however, since the robot was only actuated by two motors its ability to mimic biological gaits was
22
23 164 limited. Shaikh, Hallam and Christensen-Dalsgaard [35] used a Braitenberg vehicle to replicate lizard
24
25 165 phonotaxis in a two wheeled robot; two microphones, filtered using their ear model, were coupled
26
27 166 directly to the contralateral motor inputs. The output level from the 'ear' directly determined the speed
28
29 167 of the motor, so that the robot would rotate to face, and then move towards, a stimulus of the correct
30
31 168 frequency. This enabled continuous control of the robot's motion, an improvement over the step
32
33 169 control which resulted from having to make decisions at discrete intervals.

34
35
36
37
38
39
40 170 In the robot presented here, the analogue approach was carried out by using mechanical components
41
42 171 such as switches, rather than encoders, and only analogue, rather than digital, components, so that the
43
44 172 system moved purely on reflexes rather than logic, and the total number of electronic components was
45
46 173 kept as low as possible. Each leg is controlled using an identical circuit (shown in 1(b)): actuation is
47
48 174 provided by a 3V brushed DC motor with an integrated gearbox with a high gear ratio (RS Pro 951D
49
50 175 series) resulting in low speed, low power movements most closely analogous to the grazing gait, and low
51
52 176 backdrivability and thus low compliance to better approximate the model. The DPDT switch S_F (Knitter
53
54 177 MPBS-42H01-F14) is used to change the direction of leg movement; when it is depressed (i.e. when the
55
56
57
58
59
60

1
2
3 178 leg is in stance), the leg moves backwards, and when it is released (i.e. when the leg is in swing) the leg
4
5 179 moves forwards. The microswitches S_1 and S_2 (Omron D2F-FL3) on either side of the motor limit the
6
7 180 distance the leg can move in either direction. Unloaded legs therefore move forward until either they
8
9 181 reach the front limit, when they remain at the extreme forward position, or until they are loaded, when
10
11 182 they move backwards until they either reach the rear limit, where they remain at the extreme backward
12
13 183 position, or until they are unloaded. Power to all four legs is provided using a 9V PP3 battery, due to its
14
15 184 compact size. A step-down voltage regulator (ON Semiconductor LM2575TV-ADJG) is used to provide
16
17 185 consistent voltage and current to the motor; the output voltage $V_o = V_{ref} \left(1 + \frac{R_1}{R_2}\right)$, where V_{ref} is the
18
19 186 battery output and R_1 and R_2 are as shown in Figure 1(b). By connecting the resistor R_v across one side of
20
21 187 the S_f switch, it changes between being connected in parallel across R_1 or R_2 when S_f toggles. This makes
22
23 188 it possible to change the effective value of the ratio $\frac{R_1}{R_2}$ for each different state of S_f , and thus achieve
24
25 189 different output voltages from the regulator depending on whether the switch is depressed or not. This
26
27 190 results in faster movements when the leg is unloaded, minimising the swing time, while allowing for
28
29 191 slower, higher torque movements in stance. However, as there is no feedback control, the
30
31 192 instantaneous speed of the motors is dependent on motor mechanical load.
32
33
34
35
36
37
38
39 193 The body and legs were designed in Siemens SolidEdge and 3D printed in PLA using a MakerBot
40
41 194 Replicator 2. Each leg shares a similar basic design; however, the 'shoulders' which contact the limit
42
43 195 switches are asymmetric such that the forward reach of the front limb is mirrored in the backwards
44
45 196 reach of the ipsilateral rear limb, and the backwards reach of the front limb is mirrored in the forwards
46
47 197 reach of the ipsilateral rear limb. This prevents the feet colliding during walking. A large portion of each
48
49 198 leg is made up of S_f which acts as a contact sensor; these switches were modified from an off the shelf
50
51 199 model to have a softer and shorter spring that would be deflected by the relatively low mass of the
52
53 200 robot, and to reduce the travel of the switch so as to minimise leg compliance which would diverge from
54
55
56
57
58
59
60

1
2
3 201 the idealised 'toppling table' model. The length of the legs was also designed to prevent collisions, and
4
5 202 also to ensure that the 'toppling' motion caused large enough vertical displacements to unload or load
6
7 203 the switches at the start or end of stance.
8
9

10 204 *2.2 Experimental protocol and data analysis:*

11
12
13

14 205 A VH3 Walkway pressure mat (Tekscan Inc., Boston, MA, USA) was used to determine the forces exerted
15
16 206 by all four of the robot's feet concurrently, while a Basler acA2000-165umNIR high speed camera (Basler
17
18 207 AG, Ahrensburg, Germany) was used to video each trial. A push switch connected to a USB-6008 DAQ
19
20 208 (National Instruments, Austin, TX, USA), which sent a pulse to both instruments, was used to trigger
21
22 209 simultaneous data collection via Tekscan Walkway software v7.70 in the case of the pressure mat, and
23
24 210 custom LabView code in the case of the camera; both sets of data were collected at 100Hz. The robot
25
26 211 was placed at one end of the walkway, slightly before the edge of the sensing area. Recording was
27
28 212 triggered when the robot reached the recording area, and stopped when the robot reached the end of
29
30 213 the mat or stopped moving (e.g. because it toppled over). The best 25 videos were used for analysis.
31
32 214 Initially the robot was too light to produce usable data from the pressure mat, so 50g of wheel balance
33
34 215 weights were fixed to the underside of the body, as close to the centre as possible.
35
36
37
38

39 216 **3. Results and discussion:**

40
41

42 217 Tekscan Walkway software v7.70 was used to segment the pressure mat output into individual footfalls
43
44 218 and calculate vertical ground reaction forces (GRF), Kinovea 0.8.15 was used to digitise the high speed
45
46 219 videos and MATLAB was used to analyse the digitised data. Stride time for each leg was defined as the
47
48 220 time between two consecutive touchdowns. Duty factor was calculated for each leg as the duration of
49
50 221 contact divided by the stride time. Phase was calculated for left and right sides separately as the interval
51
52 222 between hind and fore foot touchdown times divided by median stride time for that side. Since strides
53
54 223 did not always start with the same foot, phases were converted to radians and transformed using the
55
56
57
58
59
60

224 MATLAB function 'wrapTo2Pi', for analysis; normalised values are reported here for ease of
 225 comprehension.

226 Figure 2(a) shows an example of the trajectories taken by the robot's feet; hind and forelegs display very
 227 different trajectories. The foreleg trajectories are asymmetric, initially with little vertical displacement,
 228 then lifting higher towards the end of the swing. Conversely, the hind leg trajectories are more
 229 symmetric, but with very little vertical displacement. Further examples of the robot's motion can be
 230 found in videos S2.1-2.3 in the supplementary information, along with corresponding pressure mat
 231 output. The order in which the feet move is very consistent; 82.8% of the foot transitions are from either
 232 hind foot to ipsilateral forefoot, or forefoot to contralateral hind foot, the same as in the lateral
 233 sequence walk used by most quadrupedal animals. In contrast, the stance and stride times, and hence
 234 the duty factors, display a lot of variation; average means and standard deviations are shown in Table 1
 235 below.

	LH	LF	RH	RF
Stance time (s)	0.82±0.18	0.82±0.36	0.88±0.23	0.65±0.25
Stride time (s)	1.51±0.24	1.23±0.33	1.51±0.20	1.31±0.42
Duty factor	0.54±0.10	0.64±0.15	0.60±0.11	0.49±0.12

236 *Table 1: Mean and standard deviations of stance time, stride time and duty factor for each of the legs*

237

238

239

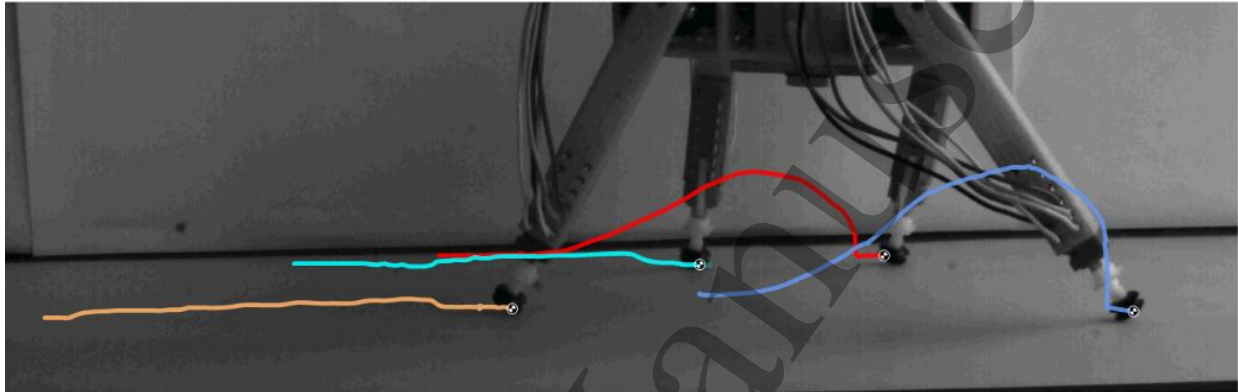
240

241

242

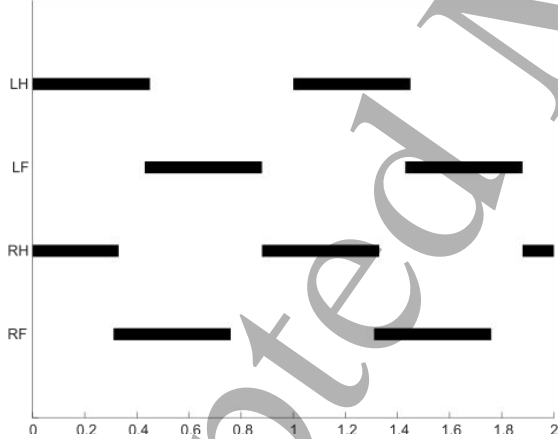
243

(a)

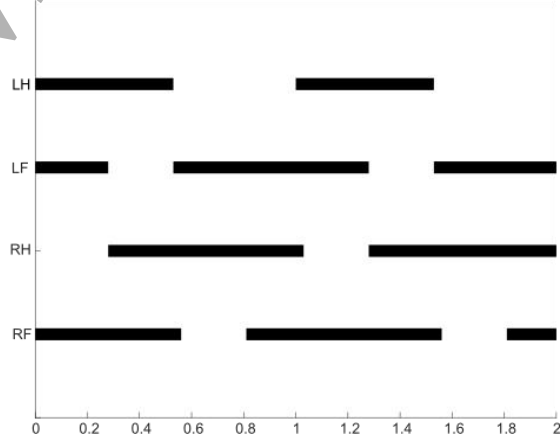


(b)

(i)



(ii)



244

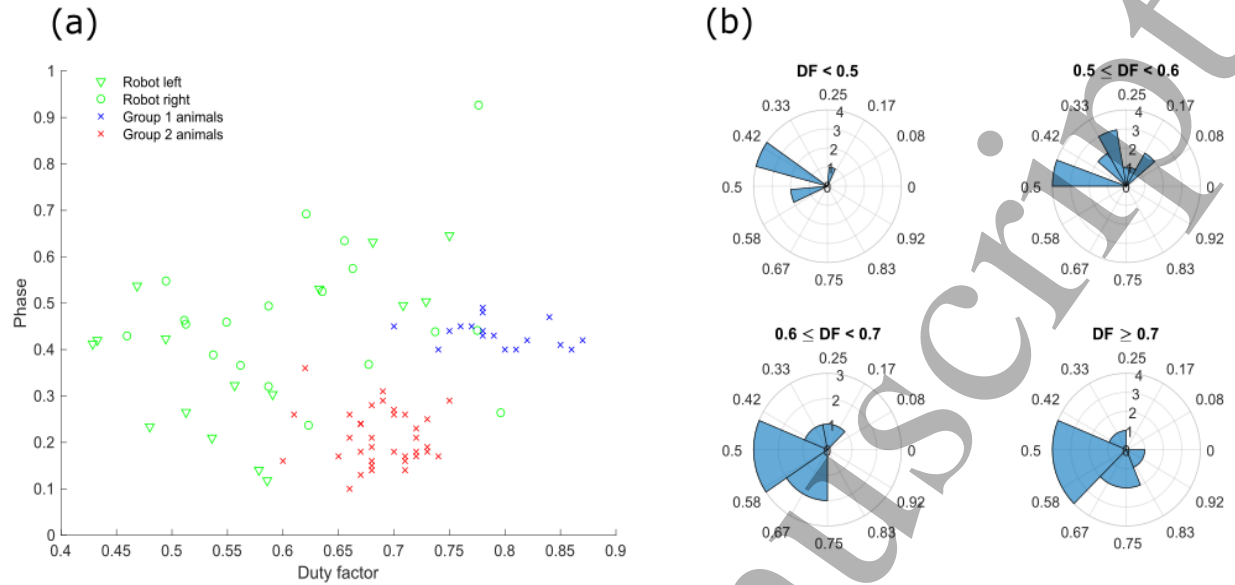
245 *Figure 2: Exemplar kinematics for the robot's gait. (a) High speed video frame showing trajectories of the*

246 *robot's feet throughout a stride, tracked using Kinovea. (b): Gait diagrams showing how the robot's walk*

247 *changes with duty factor. (i) a duty factor of 0.45m and a phase of 0.43, (ii) a duty factor of 0.75 and a*

248

phase of 0.53.

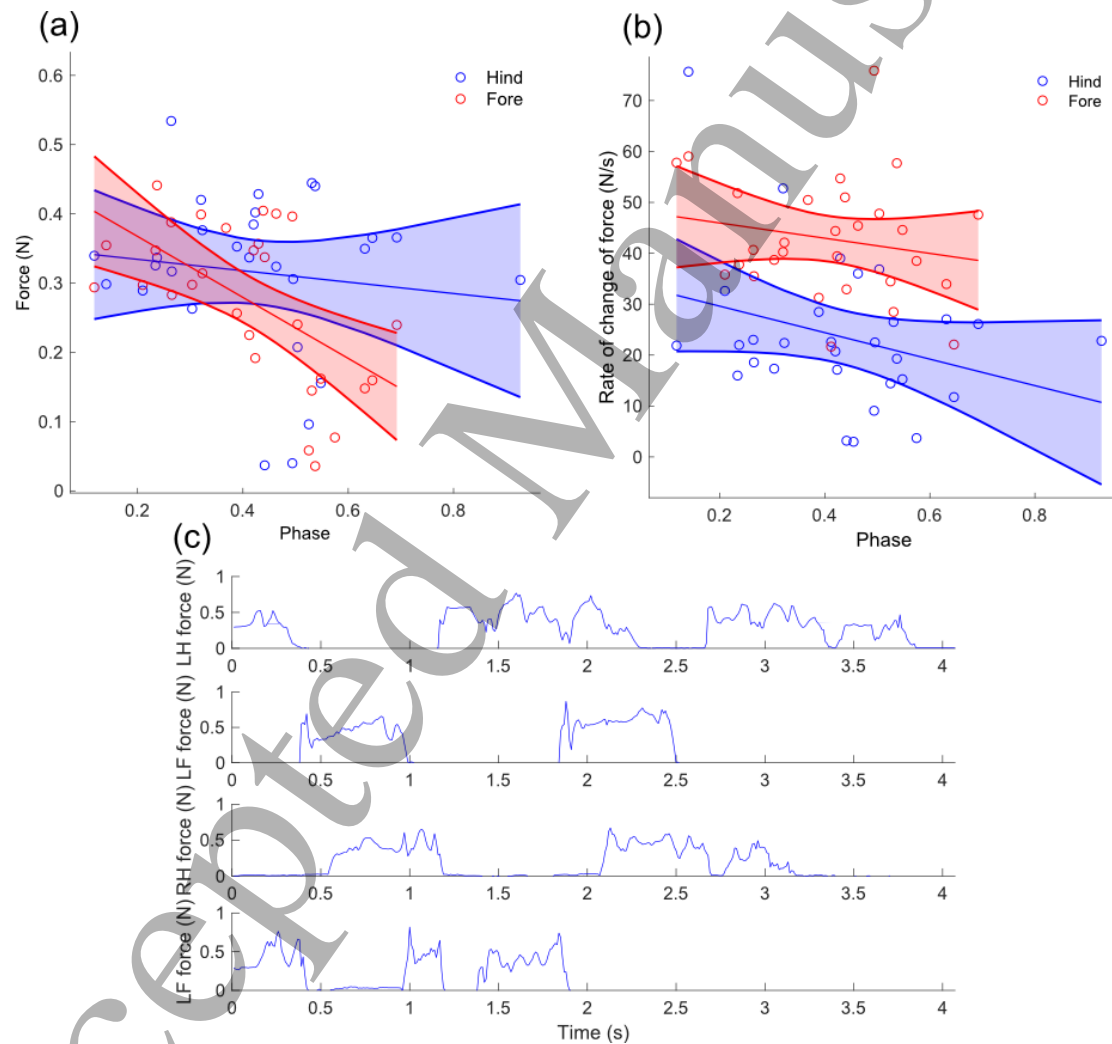


249
250 *Figure 3: The relationship between phase and duty factor (calculated as described above) in walking*
251 *animals and the robot. (a): Phase for left and right sides plotted against median duty factor for that side,*
252 *for individual strides. Values for animals and group labels are taken from [11]; group 1 animals are slow*
253 *or small and use high duty factors (e.g. hippo, mouse), while group 2 animals are more upright and use*
254 *lower duty factors (e.g. horse, dog). (b): Rose plots of phases binned by duty factor, DF, illustrating how*
255 *phases rotate around counterclockwise as duty factor increases*

256 This variation in foot timings is likely a consequence of the lack of active control making the robot very
257 sensitive to initial conditions. The robot is lifted so that all four feet are unloaded and return to their
258 extreme forward position, then it is placed on the mat with all four feet making contact almost
259 simultaneously; despite this, slight variations in foot loading or relative leg position occur at the start of
260 a trial, which then propagate through the walk cycles. Since there is no feedback control in the motors,
261 neither the speed of leg movements, nor the speed of the whole robot is constant throughout, or
262 between strides. The fact that the same foot order is used in almost every transition, despite these
263 variations, suggests that it is not dependent on stance kinematics or overall body speed, and is
264 conversant with the model presented in [11] and [31], where the relationship between phase and duty

1
2
3 265 factor is independent of absolute speed. However, one effect of the changes in timings is that while the
4
5 266 order of leg movements is the same, the relative phase of the leg movements changes with duty factor,
6
7 267 as shown in Figure 3(a). This means that at duty factors up to 0.6 the phase is mostly below 0.5,
8
9 268 however as duty factor increases the phase also increases. This can be seen more clearly when the data
10
11 269 is binned by duty factor and plotted as rose plots (Figure 3(b)); as duty factor increases the distributions
12
13 270 rotate counter clockwise from the upper quadrants to the lower left quadrant, with a modal phase of
14
15 271 0.43 at duty factors less than 0.5, to a modal phase of 0.53 at duty factors higher than 0.7. Gait diagrams
16
17 272 for these two cases are illustrated in Figure 2(b). The overall trajectory of the duty factor – phase plot
18
19 273 follows that of the animals presented in [11], but shifted so that phases are higher for a given duty
20
21 274 factor. Towards the higher end of duty factor and phase it begins to extend into the region occupied by
22
23 275 primates (which typically use a diagonal sequence walk close to 0.75 phase); however, diagonal
24
25 276 transitions (i.e. from hind to contralateral fore, or fore to ipsilateral hind) only comprised 7.4% of the
26
27 277 total number of the robot's foot movements. The gait used by the robot is more similar to the grazing
28
29 278 gait defined in [31], to the extent that it has a conserved footfall pattern with variations in stance time,
30
31 279 and phases close to 0.5, although these characteristics are also displayed at duty factors much lower
32
33 280 than 1, and the phases do not appear to be converging on 0.5, instead overshooting, particularly at
34
35 281 higher duty factors. Unlike the grazing gait, the robot's gait is not truly intermittent; while some legs
36
37 282 achieve high duty factors above 0.8 and others achieve low duty factors below 0.5, this is typically due
38
39 283 to high levels of rolling to one side or the other, rather than pauses where all four legs are on the ground
40
41 284 for high duty factors, or aerial phases for low duty factors. If the robot entered either of these states it
42
43 285 would likely signal the end of the trial, either because it would remain stationary, or because it would tip
44
45 286 over (depending on whether the positions of the feet enclosed the projection of the centre of mass to
46
47 287 the floor when they were all loaded). This tendency to roll may also explain why the phases did not
48
49 288 converge on 50%; the simplified model of the grazing gait considered only displacement of the body and
50
51
52
53
54
55
56
57
58
59
60

289 feet in two dimensions – vertical and front-rear; however, the rolling moment also produces lateral
 290 movement of the centre of mass (c.f. [36]). At the moment of foot transition in a pure 50% phase gait,
 291 the feet on one side of the robot are at their point of closest separation, while the feet on the other side
 292 are at their furthest separation. This means that the robot is particularly vulnerable to excessive rolling,
 293 and potentially tipping over sideways, resulting in a failed stride which was therefore not included in the
 294 analysis.



295

296 *Figure 4: Forces exerted by the robot's feet, thresholded to remove noise (a): Mean forces for hind and*

297 *fore feet plotted against phase. (b): Peak (maximum) rate of change for hind and fore feet plotted*

51
52
53
54
55
56
57
58
59
60

1
2
3 298 *against phase. (c): An example force trace for all four legs: LH denotes left hind foot, RH denotes right*
4
5 299 *hind, LF denotes left fore and RF denotes right fore. Discontinuities can be observed at the point of touch*
6
7
8 300 *down in the traces for the fore feet.*
9

10 301 Figures 4(a) and 4(b) show mean force, and peak rate of change of force throughout stance plotted
11
12 302 against phase for fore and hind legs. A threshold of 25mN was applied to remove noise; this level was
13
14 303 determined by recording data from the unloaded pressure mat, with the threshold set to one standard
15
16 304 deviation above the mean noise value. Mean forces are similar for fore and hind feet across phases, with
17
18 305 a decrease in peak force as phase increases, particularly in the fore limbs, which is likely due to the
19
20 306 corresponding increase in duty factor[37]. However, rate of change of force is much higher for fore
21
22 307 limbs; this corresponds to the trajectories shown in Figure 2(a), where the vertical displacement in the
23
24 308 forelimbs changes much more sharply than in the hind limbs. For both hind and fore limbs peak rates of
25
26 309 change of force decrease with increasing phase. Figure 4(c) shows a typical force trace over a stride for
27
28 310 each of the legs, and demonstrates that the high rate of change of force in the forelegs is due to a large,
29
30 311 but transient, spike in force at the beginning of stance. This corresponds to the discontinuities identified
31
32 312 in[31]; the reduction of these discontinuities at higher duty factors and phases supports the theory that
33
34 313 the grazing gait is used to minimise disruptions in weight support, and although the order of foot
35
36 314 movements is not the same as primates, it also suggests that using higher phases may be a way to
37
38 315 reduce discontinuities which would be undesirable when walking on branches. The relative timings of
39
40 316 fore and hindfoot movements also support leg loading over the stability theory; if the legs were moving
41
42 317 in a way that maximised stability margin, then a hindfoot movement would be followed immediately
43
44 318 with a forefoot movement, while the fore-hind transition would have a longer interval. This would result
45
46 319 in the feet forming a parallelogram of support. However, the mean time interval between fore-hind foot
47
48 320 movements $0.62\pm 0.33s$, much shorter than the mean interval of $1.01\pm 0.44s$ between hind-fore
49
50
51
52
53
54
55
56
57
58
59
60

321 movements, and much closer to the grazing gait where the hind limb moves directly after the forelimb,
322 forming isosceles trapeziums of support.

323 4. Conclusions:

324 In this paper we have demonstrated that it is possible to achieve quadrupedal walking using only
325 reflexes responding directly to sensor inputs, without any form of directed software controller.
326 Furthermore, we have found that this gait is similar in a number of ways to gaits found in nature; the
327 lateral sequence walk used by most animals at lower duty factors, and the 'grazing gait' used by many
328 ungulates while feeding at higher duty factors. These results provide some empirical support for the
329 theory proposed in [31]: that the grazing gait develops spontaneously from an animal's body geometry,
330 with the timing and order of foot movements determined by leg loading rather than attempting to
331 maximise stability. It was also suggested in [31] that the 'toppling table' model could also be applied to
332 primate gaits which have evolved in response to the challenges on moving on an arboreal substrate;
333 higher phases may be a tactic to ensure that any discontinuities in force occur at hind limb placement
334 (when the limb contacts substrate that has already been tested) rather than forelimb placement (when
335 the limb contacts new substrate). The results presented here may also support this hypothesis, by
336 revealing that higher phases can reduce discontinuities in force. Future manipulations, such as changing
337 the position of the robot's centre of mass, or changing the ratio of leg to body length, could be used to
338 test how well the 'toppling table' theory holds for more specific body morphologies, such as humped
339 animals like camels.

340 The similarities with the model in [31] occur despite the fact that it was impossible to reproduce the
341 model's motion exactly. For example, there is no swing phase in the model, legs simply disappear at the
342 end of stance and reappear at the beginning of the next stance; the feet of the model remain stationary
343 during stance, whereas in the robot there is some slipping; the limbs in the model move at a constant

1
2
3 344 speed, whereas in the robot the speed is dependent on limb loading; and the model reacts to changes in
4
5 345 loading instantaneously, whereas the robot's reactions are limited by the physical delays inherent in its
6
7 346 mechanical and electronic components. Although these factors may be the cause of the variations
8
9 347 observed in stance and swing times, they did not prevent the robot reproducing the gait used by the
10
11 348 model, suggesting that geometry dominates over them in terms of determining the robot's gait.
12
13
14

15 349 From a robotics perspective, our results contribute to the literature on walking robots with distributed,
16
17 350 embodied or reflexive control schemes by showing that consistent walking gaits do not need to be
18
19 351 encoded using CPGs or oscillators, and can instead emerge purely from body geometry and hardware
20
21 352 dynamics. While some controller oversight would be necessary for speed and direction control and
22
23 353 perturbation rejection, the computational load would be significantly reduced by removing the need for
24
25 354 continual step to step control.
26
27
28

29 355 **Competing interests:**

30
31 356 No competing interests declared
32
33
34
35 357
36
37 358
38

39 359 **Funding:**

40
41 360 This work was funded by Wellcome Trust Fellowship 095061/ Z/10/Z to JRU.
42
43 361
44
45
46 362
47
48
49 363
50
51
52 364
53
54
55 365
56
57
58
59
60

366 **References:**

- [1] M. Hildebrand, "The quadrupedal gaits of vertebrates.," *BioScience*, vol. 39, no. 11, p. 766, 1989.
- [2] R. M. Alexander, "Optimization and gaits in the locomotion of vertebrates," *Physiol. Rev.*, vol. 69, no. 4, pp. 1199-1227, 1989.
- [3] M. Herbin, R. Hackert, J.-P. Gasc and S. Renous, "Gait parameters of treadmill versus overground locomotion in mouse.," *Behavioural brain research*, vol. 181, no. 2, pp. 173-179, 2007.
- [4] A. I. Dagg, "The locomotion of the camel (*Camelus dromedarius*).," *Journal of Zoology*, vol. 174, no. 1, pp. 67-78, 1974.
- [5] M. Hildebrand, "Symmetrical gaits of primates.," *American Journal of Physical Anthropology*, vol. 26, no. 2, pp. 119-130, 1967.
- [6] C. J. Pennycuik, "On the running of the gnu (*Connochaetes taurinus*) and other animals.," *Journal of Experimental Biology*, vol. 63, no. 3, pp. 775-799, 1975.
- [7] L. J. Shapiro and D. A. Raichlen, "Lateral sequence walking in infant *Papio cynocephalus*: Implications for the evolution of diagonal sequence walking in primates.," *American Journal of Physical Anthropology*, vol. 126, no. 2, pp. 205-213, 2004.
- [8] R. M. Alexander, "The gaits of bipedal and quadrupedal animals.," *Int. J. Robot. Res.*, vol. 3, no. 2, pp. 49-59, 1984.
- [9] S. A. Crone, G. Zhong, R. Harris-Warwick and K. Sharma, "In mice lacking V2a interneurons, gait depends on speed of locomotion.," *Journal of Neuroscience*, vol. 29, no. 21, pp. 7098-7109, 2009.
- [10] D. F. Hoyt and C. R. Taylor, "Gait and the energetics of locomotion in horses.," *Nature*, vol. 292, no. 5820, p. 239, 1981.
- [11] J. R. Usherwood and Z. T. Self Davies, "Work minimization accounts for footfall phasing in slow quadrupedal gaits.," *eLife*, vol. 6, p. e29495, 2017.
- [12] M. Cartmill, P. Lemelin and D. Schmitt, "Support polygons and symmetrical gaits in mammals.," *Zoological Journal of the Linnean Society*, vol. 136, no. 3, pp. 401-420, 2002.
- [13] T. M. Griffin, R. Kram, S. J. Wickler and D. F. Hoyt, "Biomechanical and energetic determinants of the walk-trot transition in horses.," *Journal of Experimental Biology*, vol. 207, no. 24, pp. 4215-4223, 2004.

- 1
2
3 [14] C. Farley and C. Taylor, "A mechanical trigger for the trot-gallop transition in horses.," *Science.*, vol.
4 253, no. 5017, pp. 306-308, 1991.
5
6
7 [15] A. A. Biewener, "Allometry of quadrupedal locomotion: the scaling of duty factor, bonecurvature
8 and limb orientatation to body size.," *Journal of Experimental Biology*, vol. 105, pp. 147-171, 1983.
9
10 [16] J. R. Usherwood, "An extension to the collisional model of the energetic cost of support
11 qualitatively explains trotting and the trot-canter transition.," *Journal of Experimental Zoology*, vol.
12 1, no. 11, 2019.
13
14 [17] J. J. Collins and I. N. Stewart, "Coupled nonlinear oscillators and the symmetries of animal gaits.,"
15 *Journal of Nonlinear Science*, vol. 3, no. 1, pp. 349-392, 1993.
16
17 [18] S. Aoi, T. Yamashita and K. Tsuchiya, "Hysteresis in the gait transition of a quadruped investigated
18 using simple body mechanical and oscillator network models.," *Physical Review E*, vol. 83, no. 6, p.
19 061909, 2011.
20
21 [19] N. Harischandra, J. Knuesel, A. Kozlov, J.-M. Cabelguen, A. J. Ijspeert and Ö. Ekeberg, "Sensory
22 feedback plays a significant role in generating walking gait and in gait transition in salamanders: a
23 simulation study.," *Frontiers in neurorobotics*, vol. 5, p. 3, 2011.
24
25 [20] T. G. Brown, "The intrinsic factors in the act of progression in themammal.," *Proceedings of the*
26 *Royal Society B*, vol. 84, p. 308–319, 1911.
27
28 [21] S. Grillner and P. Wallen, "Central pattern generators for locomotion, with special reference to
29 vertebrates.," *Annual review of neuroscience*, vol. 8, no. 1, pp. 233-261, 1985.
30
31 [22] J. Duysens and K. Pearson, "Inhibition of flexor burst generation by loading ankle extensor muscles
32 in walking cats.," *Brain research*, vol. 187, no. 2, pp. 321-332, 1980.
33
34 [23] Y. Fukuoka, Y. Habu and T. Fukui, "A simple rule for quadrupedal gait generation determined by leg
35 loading feedback: a modeling study.," *Scientific reports*, vol. 5, p. 8169, 2015.
36
37 [24] C. Maufroy, H. Kimura and K. Takase, "Integration of posture and rhythmic motion controlsin
38 quadrupedal dynamic walking using phase modulations based on leg loading/unloading.,"
39 *Autonomous robots*, vol. 28, no. 3, pp. 331-353, 2010.
40
41 [25] H. Kimura, Y. Fukuoka and A. H. Cohen, "Adaptive Dynamic Walking of a Quadruped Robot," *The*
42 *International Journal of Robotics Research*, vol. 26, no. 5, pp. 475-490, 2007.
43
44 [26] D. Owaki, T. Kano, K. Nagasawa, A. Tero and A. Ishiguro, "Simple robot suggests physical interlimb
45 communication is essential for quadruped walking.," *Journal of The Royal Society Interface*, vol. 10,
46 no. 78, p. 20120669, 2013.
47
48
49
50
51
52
53
54
55
56
57
58
59
60

- 1
2
3 [27] D. Owaki and A. Ishiguro, "A quadruped robot exhibiting spontaneous gait transitions from walking
4 to trotting to galloping.," *Scientific reports*, vol. 7, no. 1, p. 277, 2017.
5
6
7 [28] B. Zhong, Y. O. Aydin, C. Gong, G. Sartoretti, Y. Wu, J. Rieser, H. Xing, J. Rankin, K. Michel, A. Nieceza,
8 J. Hutchinson, D. Goldman and H. Choset, "Coordination of back bending and leg movements for
9 quadrupedal locomotion," in *Robotics: Science and Systems*, Pittsburgh, PA, USA, 2018.
10
11
12 [29] A. Sprowitz, A. Tuleu, M. Vespignani, M. Ajalloeian, E. Badri and A. J. Ijspeert, "Towards Dynamic
13 Trot Gait Locomotion: Design, Control, and Experiments with Cheetahcub, Compliant Quadruped
14 Robot," *International Journal of Robotics*, vol. 32, no. 8, pp. 933- 951, 2013.
15
16
17 [30] J. Degraeve, K. Caluwaerts, J. Dambre and F. Wyffels, "Developing an Embodied Gait on a Compliant
18 Quadrupedal Robot," in *IEEE/RSJ International Conference on Intelligent Robots and Systems (IROS)*,
19 Hamburg, Germany, 2015.
20
21
22 [31] J. R. Usherwood and B. J. Smith, "The grazing gait, and implications of toppling table geometry for
23 primate footfall sequences.," *Biology letters*, vol. 14, no. 5, p. 20180137, 2018.
24
25
26 [32] M. W. Tilden, "The Design of "Living" Biomech Machines: How low can one go?," Physics Division,
27 Los Álamos National Laboratory, Los Álamos, NM, USA, 1997.
28
29
30 [33] V. Braitenberg, *Vehicles: Experiments in synthetic psychology.*, Cambridge, MA, USA: MIT Press,
31 1986.
32
33 [34] S. Still and M. W. Tilden, "Controller for a four-legged walking machine.," in *Neuromorphic Systems:
34 Engineering silicon from neurobiology*, Singapore, World Scientific, 1998, pp. 138-148.
35
36
37 [35] D. Shaikh, J. Hallam and J. Christensen-Dalsgaard, "From "ear" to there: a review of biorobotic
38 models of auditory processing in lizards.," *Biological cybernetics*, vol. 110, no. 4-5, pp. 303-317,
39 2016.
40
41
42 [36] H. Kimura, I. Shimoyama and H. Miura, "Dynamics in the dynamic walk of a quadruped robot,"
43 *Advanced robotics*, vol. 4, no. 3, pp. 283-301, 1989.
44
45
46 [37] T. Witte, K. Knill and A. Wilson, "Determination of peak vertical ground reaction force," *J. Exp. Biol.*,
47 vol. 207, no. 21, pp. 3639-3648, 2004.
48
49
50 [38] P. Berens, "CircStat: a MATLAB toolbox for circular statistics.," *Journal of statistical software*, vol.
51 31, no. 10, pp. 1-21, 2009.
52
53
54 [39] P. A. Bhounsule, J. Cortell, A. Grewal, B. Hendriksen, Karssen, J. D. C. Paul and A. Ruina, "Low-
55 bandwidth reflex-based control for lower power," *The International Journal of Robotics Research*,
56
57
58
59
60

1
2
3 vol. 33, no. 10, pp. 1305-1321, 2014.
4

5
6 367

7
8 368

9
10
11 369
12
13
14
15
16
17
18
19
20
21
22
23
24
25
26
27
28
29
30
31
32
33
34
35
36
37
38
39
40
41
42
43
44
45
46
47
48
49
50
51
52
53
54
55
56
57
58
59
60

Accepted Manuscript